

A Rabbit Model for Testing Helper-Dependent Adenovirus-Mediated Gene Therapy for Vein Graft Atherosclerosis

Lianxiang Bi,¹ Bradley K. Wacker,¹ Emma Bueren,¹ Ervin Ham,¹ Nagadhara Dronadula,¹ and David A. Dichek¹

¹Division of Cardiology, Department of Medicine, University of Washington, Seattle, WA 98195, USA

Coronary artery bypass vein grafts are a mainstay of therapy for human atherosclerosis. Unfortunately, the long-term patency of vein grafts is limited by accelerated atherosclerosis. Gene therapy, directed at the vein graft wall, is a promising approach for preventing vein graft atherosclerosis. Because helper-dependent adenovirus (HDAd) efficiently transduces grafted veins and confers long-term transgene expression, HDAd is an excellent candidate for delivery of vein graft-targeted gene therapy. We developed a model of vein graft atherosclerosis in fat-fed rabbits and demonstrated long-term (≥ 20 weeks) persistence of HDAd genomes after graft transduction. This model enables quantitation of vein graft hemodynamics, wall structure, lipid accumulation, cellularity, vector persistence, and inflammatory markers on a single graft. Time-course experiments identified 12 weeks after transduction as an optimal time to measure efficacy of gene therapy on the critical variables of lipid and macrophage accumulation. We also used chow-fed rabbits to test whether HDAd infusion in vein grafts promotes intimal growth and inflammation. HDAd did not increase intimal growth, but had moderate—yet significant—pro-inflammatory effects. The vein graft atherosclerosis model will be useful for testing HDAd-mediated gene therapy; however, pro-inflammatory effects of HDAd remain a concern in developing HDAd as a therapy for vein graft disease.

INTRODUCTION

Heart disease, due largely to atherosclerosis, remains the leading cause of death in the United States and throughout the world.^{1,2} The morbidity and mortality of atherosclerosis are due primarily to involvement of the coronary arteries, in which accumulation of intimal lipid and inflammatory cells leads to lumen narrowing, diminished blood flow, and thrombotic occlusion, along with associated symptoms of chest pain, myocardial infarction, heart failure, and sudden death.^{3,4} Despite advances in medical therapy and percutaneous coronary interventions (e.g., angioplasty and stenting), coronary artery bypass grafting (CABG) surgery remains a mainstay of therapy for severe coronary artery disease.^{5–7} Accordingly, approximately 400,000 CABG surgeries are performed annually in the United States.⁸ However, the long-term benefits of CABG are limited by a high rate of occlusion of the saphenous vein segments that are used to construct coronary bypass grafts.⁹ Coronary artery bypass

vein graft patency is estimated at 80%–90% at 1 year and 50% at 10 years,^{10,11} with the progressive loss of patency due largely to development of vein graft atherosclerosis.^{10,12,13}

Current therapy to prevent vein graft atherosclerosis is essentially limited to lipid-lowering drugs, typically statins.^{14,15} Statin therapy is implemented in the vast majority of CABG recipients;¹⁶ however, there is no evidence that widespread statin use has increased vein graft patency rates over time, and there is some evidence that patency rates are decreasing.⁹ Moreover, statin therapy appears to be effective only up to a point: statin-induced reduction of LDL cholesterol to <100 mg/dL increased vein graft patency; however, further reduction to <70 mg/dL had no additional benefit.¹⁷ Vein graft atherosclerosis can be avoided by use of arterial bypass grafts, such as the left internal thoracic artery, which has a 10-year patency rate of $>95\%$.¹⁸ However, there is only 1 left internal thoracic artery in any single CABG candidate and essentially all CABG candidates require more than 1 bypass conduit.^{5,16} Use of both the left and right internal thoracic arteries for bypass grafting does not improve cardiovascular outcomes when compared to use of only the left internal thoracic artery, along with a vein graft, and is associated with a significant increase in sternal wound infections.¹⁹ Radial arteries are also occasionally used as CABG conduits; however, their long-term patency rates and associated clinical outcomes are no better than those obtained with vein grafts.^{20,21}

We, and others, have proposed gene therapy as a promising approach for prevention of vein graft atherosclerosis.^{22,23} Gene therapy for vein graft atherosclerosis would consist of expressing a therapeutic gene in the graft itself, with the gene chosen for its ability to prevent lipid accumulation, inflammation, or vascular remodeling that is thought to predispose to rapid development of atherosclerosis.^{24,25} However, progress toward developing gene therapy for vein graft atherosclerosis was long limited by the need for durable transgene expression, which is likely required to prevent a disease that develops and

Received 2 July 2017; accepted 21 September 2017;
<https://doi.org/10.1016/j.omtm.2017.09.004>.

Correspondence: David A. Dichek, University of Washington, 1959 NE Pacific St., P.O. Box 357710, Seattle, WA 98195-7710, USA.

E-mail: ddichek@uw.edu

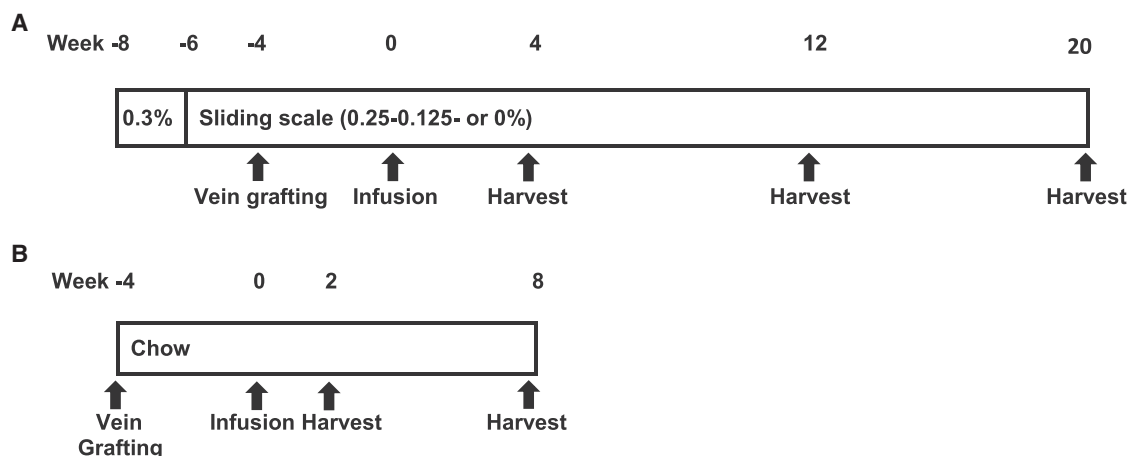


Figure 1. Study Protocols

(A) Vein graft atherosclerosis study. Rabbits were begun on a 0.3% cholesterol diet. Their plasma cholesterol levels were measured after 2 weeks on diet and every 2 weeks thereafter. On the basis of these measurements, the cholesterol content of each rabbit's diet was adjusted (0.25%, 0.125%, or 0% cholesterol), with a goal of achieving plasma cholesterol levels of 200–800 mg/dL. Vein grafts were placed after 4 weeks of high-fat diet, HDAdNull was infused into the grafts 4 weeks later, and the grafts were harvested 4, 12, or 20 weeks after HDAdNull infusion. (B) Vein graft inflammation study. Vein grafts were placed in chow-fed rabbits. 4 weeks later, grafts were infused with vehicle (DMEM), HDAdNull, or FGAdNull. Grafts were harvested either 2 or 8 weeks later.

progresses over many years. We recently reported that transduction of vein grafts of chow-fed rabbits with a helper-dependent adenoviral (HDAd) vector yielded expression of a transgene for at least 24 weeks, with stable expression from 4 weeks onward.²⁶ Transduction of arteries of chow-fed rabbits with the same HDAd achieved transgene expression for at least 48 weeks, also with stability after 4 weeks.²⁷ Because HDAd appears capable of mediating durable—if not indefinite—transgene expression in blood vessels, HDAd is a promising vector for developing gene therapy for vein graft atherosclerosis. However, testing of HDAd for this purpose requires an animal model of vein graft atherosclerosis as well as evidence that HDAd persists in the vein graft wall during atherosclerosis development.

Here, we report the use of cholesterol-fed rabbits to develop a reproducible and quantitative animal model that can be used for testing HDAd-mediated gene therapy for vein graft atherosclerosis. In a separate series of experiments, performed in chow-fed rabbits, we also tested whether HDAd infusion to grafted veins causes vein graft wall inflammation and intimal growth.^{28–30}

RESULTS

Cholesterol Levels, Surgical Procedures, and Vein Graft Patency in Fat-Fed Rabbits

To generate hyperlipidemia (which is required for the development of vein graft atherosclerosis),³¹ 18 rabbits were fed a high-fat diet, beginning with 0.3% cholesterol (Figure 1A). As expected,^{31–33} response to the high-fat diet was heterogeneous with plasma cholesterol levels after 2 weeks, ranging from 78 to 930 mg/dL (Figure 2 and data not shown). By adjusting dietary cholesterol every 2 weeks, plasma cholesterol levels were maintained within a relatively narrow range (mean, 400–700 mg/dL) for the duration of the study. After

4 weeks of high-fat diet, all rabbits underwent bilateral placement of end-to-side external jugular vein-to-common carotid artery interposition grafts. Transcutaneous ultrasonography performed 5–7 days later (Figure S1) revealed that 34 of the 36 vein grafts (94%) were patent, with unilateral occlusions in 2 rabbits. 4 weeks after graft placement, all 18 rabbits underwent re-operation for vein graft transduction. We delayed transduction until 4 weeks after grafting because transduction at the time of grafting leads to rapid loss of transgene expression, whereas delayed transduction yields durable transgene expression.²⁶

During the transduction surgery, 2 rabbits (both with 2 patent grafts) died from anesthesia complications. The remaining 16 rabbits (with 30 patent grafts) underwent successful vein graft transduction, including exposure of the grafts, temporary occlusion, and intraluminal infusion with an HDAd containing an empty expression cassette (HDAdNull).³⁴ One rabbit (with 2 patent grafts) was euthanized due to respiratory distress on postoperative day 2 after infusion. Transcutaneous ultrasound performed 5–7 days later revealed that 27 of the 28 remaining transduced grafts (96%) were patent. The grafts were harvested 4, 12, or 20 weeks later, with patency preserved in all 27 grafts. We harvested grafts at multiple time points in order to determine the time course during which atherosclerosis develops in HDAd-infused vein grafts and evaluate the magnitude and reproducibility of quantitative measurements of atherosclerosis (e.g., lipid and macrophage accumulation, inflammatory markers, intimal growth, lumen diameter, and percent lumen stenosis) at various time points. These data are required to enable design of future studies in which a therapeutic transgene expressed from HDAd would be tested for its ability to prevent vein graft atherosclerosis.

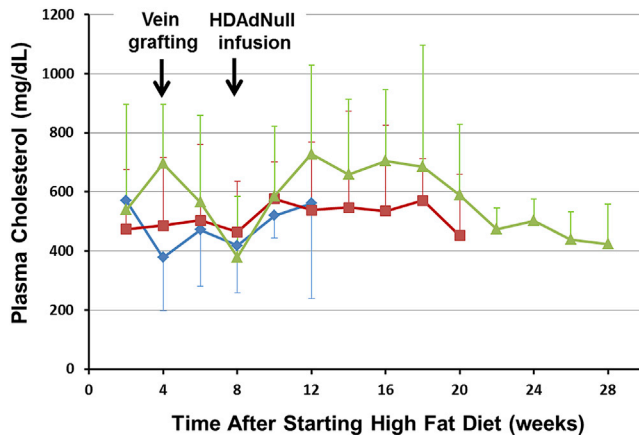


Figure 2. Plasma Cholesterol Concentrations in Rabbits Fed a High-Fat Diet Vein graft surgery was performed after 4 weeks on diet, with HDAdNull infusion 4 weeks later. Rabbits are separated into 3 cohorts based on time of harvest (4, 12, or 20 weeks after vector infusion, with data represented in blue, red, and green, respectively). Data are mean \pm SD.

In Vivo Vein Graft Diameters and Hemodynamics

At the time of harvest, we used transcutaneous ultrasonography to measure lumen diameters in 14 of the 27 patent vein grafts. The remaining 13 grafts were not measured due to lack of available equipment. Measurements were made under general anesthesia before beginning the harvest surgery. Mean lumen diameters ranged from 5.2 mm to 6.0 mm, yielding calculated mean lumen areas from 22.3 to 28.6 mm² (Table S1). Lumen diameters (and areas) tended to be higher at 20 weeks compared to the earlier time points. After surgical exposure of the grafts, we used an external probe to measure blood flow in 23 of the 27 grafts (the flow meter was unavailable for 4 grafts). We measured flow—and calculated pulsatility and shear—because these hemodynamic properties affect inflammation and atherosclerosis development^{35–37} and therefore cannot be left as unknown (and uncontrolled) variables in atherosclerosis models. No flow measurements were made in both grafts of two rabbits due to technical issues (lack of equipment for measuring instantaneous flow in one case and rapid hemodynamic decompensation under anesthesia in the other). Mean vein graft blood flows ranged from 19.8 to 25.6 mL/min (Table S1). We later assessed baseline blood flow in ungrafted common carotids using chow-fed rabbits enrolled in a separate study; see below. These flow measurements were made on anesthetized rabbits immediately before vein graft placement. Mean flow ($n = 11$) was 34 ± 9.2 mL/min in the left carotid and 35 ± 11.4 mL/min in the right carotid. We calculated pulsatility in 16 of 27 vein grafts. No pulsatility calculations were made in 9 grafts (5 rabbits) due to lack of equipment (flow probe, chart recorder, or both) and in 2 grafts (1 rabbit) due to rapid hemodynamic decompensation under anesthesia. Mean pulsatility index ranged from 2.9 to 4.9, with a trend toward lower values at 20 weeks (Table S1). For the 12 grafts for which we had both blood flow and diameter measurements, we calculated laminar shear stress. Mean laminar shear stress ranged from 1.2 to 1.8 dynes/cm², with a trend toward lower shear stress at 20 weeks (Table S1).

Presence of Vector DNA and Expression of Inflammatory Cytokines

Vector genomes were detected in all 27 patent grafts (Figure 3A), with the number of genomes/vascular wall cell declining from 0.36 ± 0.31 at 4 weeks to 0.08 ± 0.05 at 20 weeks ($p = 0.04$). In our previous work and in results reported by others, incubation of adenovirus in a vein lumen followed by grafting of the vein results in transgene expression that is largely confined to luminal endothelial cells.^{26,38–41} Other groups have reported transgene expression in the venous media and adventitia, but this may be due to variability in technique.^{42–44} Based on our previous work with vein grafts of chow-fed rabbits²⁶ and our finding that hyperlipidemia does not alter the endothelial predominance of transgene expression in adenovirus-infused arteries,²⁹ we assume that most HDAdNull genomes (if they are intracellular) are likely within luminal endothelial cells. By counting endothelial and total vascular wall nuclei in graft histologic sections, we determined that endothelial cells comprise $\sim 2\%$ of total vascular wall cells at all 3 time points (data not shown). Therefore, vector genomes per endothelial cell were 18.1 ± 15.7 at 4 weeks, 7.3 ± 7.0 at 12 weeks, and 3.9 ± 2.6 at 20 weeks (if endothelial cells represent only 50% of the transduced cells, these values decrease proportionately). Inflammatory cytokines contribute to atherogenesis,⁴⁵ and their expression levels can be a target for therapy or a measure of therapeutic efficacy. Accordingly, we measured mRNA for the atherogenic cytokines monocyte chemoattractant protein-1 (MCP-1), interleukin-1 β (IL-1 β), IL-6, tumor necrosis factor alpha (TNF- α), and interferon- γ (IFN- γ) (Figures 3B–3F). Expression of IFN- γ was far lower at 12 and 20 weeks versus 4 weeks ($p \leq 0.008$); expression of IL-1 β declined between 4 and 12 weeks ($p = 0.004$) and then trended upward. Expression of MCP-1, IL-6, and TNF- α all tended to decrease between 4 and 12 weeks, remaining stable or trending upward at 20 weeks.

Vein Graft Morphometry, Histology, and Lipid Content

To assess the kinetics of intimal growth and determine whether intimal growth was associated with lumen narrowing, we examined histologic sections of the 27 patent grafts. One of the 4-week grafts was excluded from analysis of wall structure because 2 of 3 segments contained valves, distorting the neointimal area. Whereas the intima of an ungrafted rabbit external jugular vein from a chow-fed rabbit is limited to a single layer of endothelium, a large neointima was present in all of the 26 grafts we examined (Figures S2B–S2D and S2F–S2H; compare to the ungrafted vein in Figures S2A and S2E). There was a tendency for the neointimal area to increase at later time points (Figure 4A). Medial areas were similar at 4 and 12 weeks and larger at 20 weeks ($p = 0.02$; Figure 4B). Intima/media area ratio was substantial at 4 weeks (2.6 ± 0.8), with nominal changes at 12 and 20 weeks (Figure 4C). Vein graft lumen diameters (and areas) tended to increase modestly over time (Figures 4D and 4E). Percent lumen stenosis was similar ($\sim 40\%$) at all 3 time points (Figure 4F).

We analyzed the intimal composition of all 27 patent grafts. Vein graft atherosclerosis is thought to be driven largely by accumulation

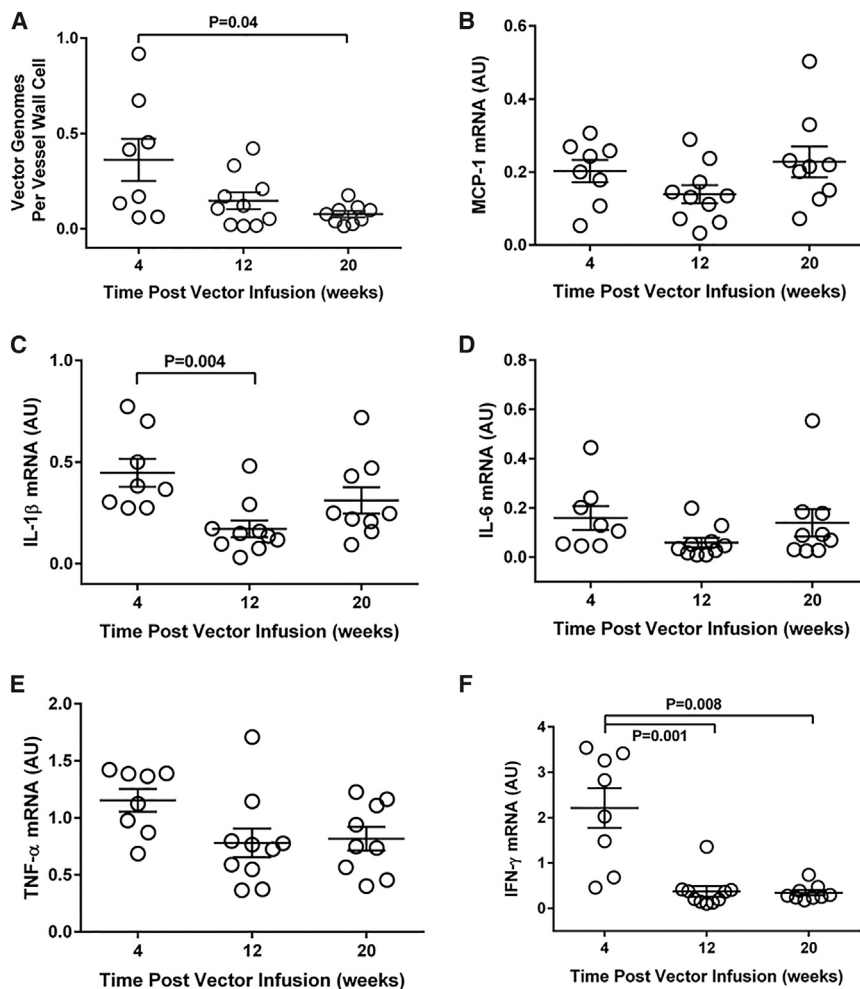


Figure 3. Vector Genomes and Inflammatory Cytokine Expression in Vein Grafts Harvested from Hyperlipidemic Rabbits

DNA and RNA were extracted from vein grafts harvested 4 (n = 8), 12 (n = 10), or 20 weeks (n = 9) after HDAdNull infusion. (A) Vector DNA was measured by qPCR. (B–F) Levels of mRNA encoding (B) MCP-1, (C) IL-1 β , (D) IL-6, (E) TNF- α , and (F) IFN- γ were measured with qRT-mediated PCR, with normalization to GAPDH mRNA in the same samples. AU, arbitrary units. Data points are individual grafts; bars are group means \pm SEM. p values are from ANOVA, with correction for pairwise post hoc comparisons.

We also measured vein graft cholesterol accumulation with mass spectrometry performed on extracts of full-thickness grafts. Vein graft total cholesterol content increased by approximately 80% between 4 and 12 weeks (p = 0.02) and then stabilized (Figure 5F). Similar patterns over time were detected for both unesterified cholesterol and total cholesteryl esters (Figures S5E and S5F). The percentage of total cholesterol that was esterified was constant over time (~70%, Figure S5G).

Surgical Procedures, Vein Graft Patency, and Hemodynamics in Chow-Fed Rabbits

In a separate series of experiments, we tested whether infusion of HDAdNull into grafted veins promotes inflammation and intimal growth, as we (and others) have reported after

infusion of both first-generation (FG) Ad and HDAd into arteries.^{28–30,46,47} To increase the sensitivity of our assays to detect HDAdNull-induced inflammation and intimal growth, we performed these experiments with chow-fed rabbits (in which we anticipated less baseline inflammation and intimal growth than in vein grafts of hyperlipidemic rabbits).³¹ The primary goal of these experiments was to test the hypothesis that—compared to infusion of DMEM vehicle—infusion of HDAdNull did not increase inflammation and intimal growth. As a positive control for pro-inflammatory effects and intimal growth,³⁰ we included a group of first-generation null adenoviral vector (FGAdNull)-infused vein grafts. However, the a priori experimental design mandated that only the DMEM and HDAdNull groups were compared formally.

Rabbits enrolled in the study (n = 29; Figure 1B) received bilateral external jugular vein-to-common carotid artery interposition grafts. Transcutaneous ultrasonography 5–7 days after grafting showed 58 of 58 (100%) of the grafts were patent. One rabbit was removed from the study because of a febrile illness. 4 weeks after grafting,

of intimal lipid and macrophage-derived foam cells;¹³ therefore, we expected that the vein graft intimas would be relatively rich in lipid and macrophages as well as adhesion molecules that mediate monocyte-macrophage recruitment. Only a small amount of vein graft intimal area (~1% to 2% at all time points) stained positively for muscle actin (a marker of smooth muscle cells; Figures 5A and S3B–S3D). A far larger percentage of intimal area (~20%–40%) stained positively for the macrophage marker RAM-11 (Figures 5B and S3F–S3H). RAM-11-stained intimal area tended to increase between 4 and 12 weeks and then stabilize. Intercellular adhesion molecule-1 (ICAM-1) (Figures 5C and S4B–S4D) and vascular cell adhesion molecule-1 (VCAM-1) (Figures 5D and S4F–S4H) were both present in the graft intimas. ICAM-1 expression was initially low but increased significantly over time (p = 0.001), whereas VCAM-1 was present at low levels at all time points. Oil red O staining revealed substantial lipid accumulation (~10%–30% of intimal area) in all vein grafts. The percentage of oil-red-O-stained intimal area increased by ~50% between 4 and 12 weeks (p = 0.02), with a similar amount of oil-red-O-stained area at both 12 and 20 weeks (Figures 5E and S5B–S5D).

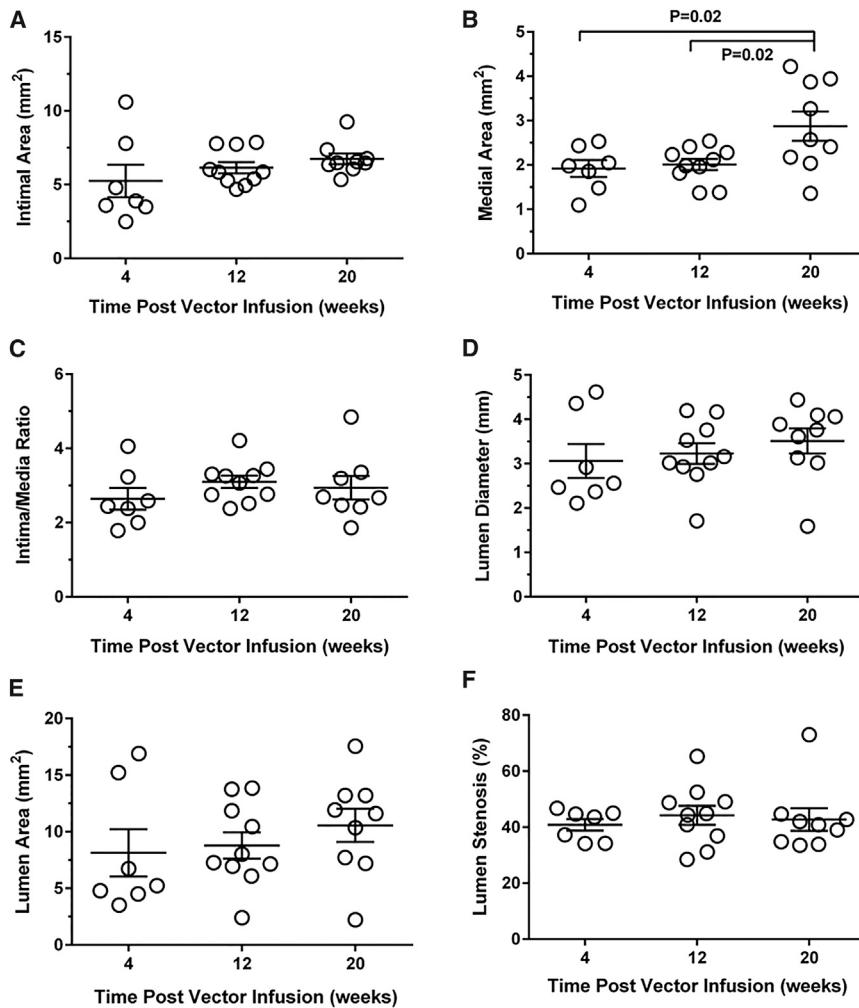


Figure 4. Morphometry of Vein Grafts Harvested from Hyperlipidemic Rabbits

Grafts were harvested 4 ($n = 7$), 12 ($n = 10$), or 20 weeks ($n = 9$) after HDAdNull infusion. Three segments of each of the grafts were embedded, sectioned, and stained with Verhoef van Gieson stain. Images of stained sections were analyzed with computer-assisted planimetry to determine (A) intimal area, (B) medial area, (C) intima/media area ratio, (D) lumen diameter, (E) lumen area, and (F) percent lumen stenosis. Data points are values for individual grafts; bars are group means \pm SEM. p values are from ANOVA, with correction for pairwise post hoc comparisons (see also Figure S2).

At harvest (2 or 8 weeks after infusion), we used transcutaneous ultrasonography to measure vein graft lumen diameters in 43 of the 49 grafts (6 grafts were not measured due to lack of equipment). Neither lumen diameters nor calculated lumen areas differed significantly between DMEM- and HDAdNull-infused grafts (Table S3; $p > 0.2$ for both measurements at both time points). All grafts were patent at harvest (either 2 or 8 weeks after infusion) based on ultrasound examination or on presence of a palpable pulse and luminal blood. After surgical exposure, we measured blood flow in 43 of the 49 grafts. For 4 grafts in 2 rabbits, instruments were unavailable and 1 graft in each of 2 rabbits ruptured during dissection. Mean flow did not differ significantly between DMEM and HDAdNull-infused grafts (Table S3; $p > 0.2$ at both time points). Pulsatility was similar

in DMEM- and HDAdNull-infused grafts at 2 weeks; however, pulsatility was significantly lower in HDAdNull-infused grafts at 8 weeks (40% lower; Table S3; $p = 0.01$). Laminar shear stress was similar between the 2 groups at both time points (Table S3; $p > 0.2$).

the rabbits remaining in the study were returned to the operating room and their grafts ($n = 56$) were exposed surgically. One rabbit was found to have a subcutaneous neck abscess and was removed from the study. Flow in 3 of the grafts was sluggish (<10 mL/min). These grafts were considered to be technical failures and were excluded from the study. The remaining grafts in which we measured flow (39 of the 51 grafts; equipment was not available for flow measurements in 12 grafts) had brisk pulsatile flow (40 ± 15 mL/min), with no significant differences in hemodynamic variables between grafts assigned to DMEM versus HDAdNull infusion (Table S2). All 51 grafts were transiently occluded, rinsed intraluminally with DMEM, and infused with DMEM, HDAdNull, or FGAdNull. The same infusate was used for both sides of the same rabbit. One rabbit died 3 hr post infusion of DMEM due to general anesthesia complications. All 49 remaining grafts (in 26 rabbits) were patent by transcutaneous ultrasonography performed 5–7 days after infusion. All of these 49 grafts completed the study and underwent hemodynamic ($n = 43$), molecular ($n = 49$), and histologic ($n = 45$) analyses.

in DMEM- and HDAdNull-infused grafts at 2 weeks; however, pulsatility was significantly lower in HDAdNull-infused grafts at 8 weeks (40% lower; Table S3; $p = 0.01$). Laminar shear stress was similar between the 2 groups at both time points (Table S3; $p > 0.2$).

Presence of Vector DNA and Expression of Inflammatory Cytokines

We measured vector DNA and cytokine RNA in extracts of 49 grafts. As expected, no vector DNA was detected in DMEM-infused vein grafts (Figure 6). In contrast, vector DNA was present in all HDAdNull-infused grafts, with equivalent levels at 2 and 8 weeks. Vector DNA was not detected in any of the FGAdNull-infused grafts (<0.01 copy per vessel wall cell or <0.5 copies per endothelial cell based on the limit of detection). Compared to DMEM-infused grafts, HDAdNull-infused grafts had significantly higher expression of IFN- γ at 2 weeks (2.6-fold; $p = 0.01$) and increased expression of IFN- γ , IL-1 β , IL-6, TNF- α , and MCP-1 at 8 weeks (2- to 4-fold; $p < 0.05$ for all; Figure 6).

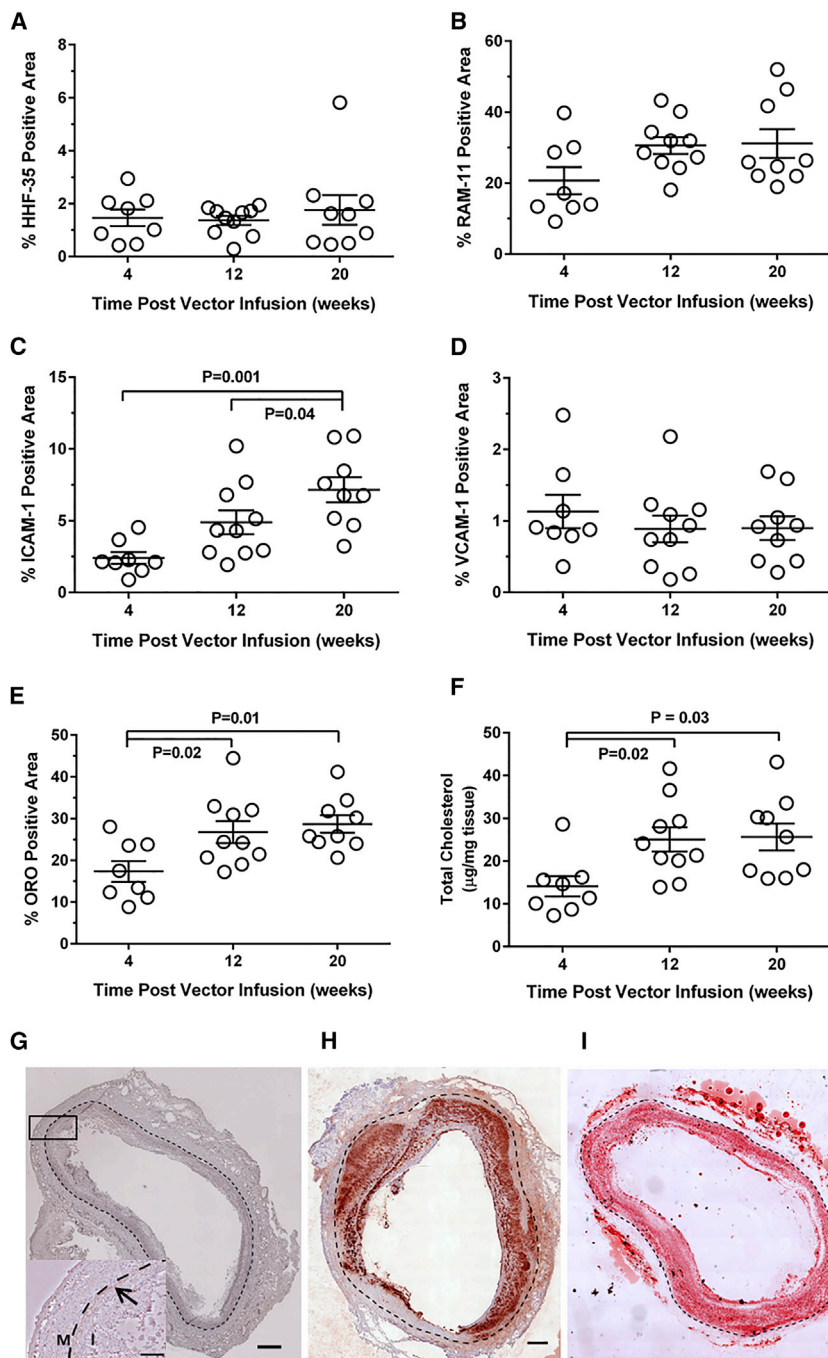


Figure 5. Cellularity, Adhesion Molecule Expression, and Lipid Accumulation in Vein Grafts Harvested from Hyperlipidemic Rabbits

Grafts were harvested 4 (n = 8), 12 (n = 10), or 20 weeks (n = 9) after HDAdNull infusion. (A–E) Three segments of each of the grafts were embedded, sectioned, and stained with antibodies or oil red O. Images of stained sections were analyzed with computer-assisted planimetry to determine the percentage of intimal area stained for (A) muscle actin (HHF-35 antibody); (B) macrophages (RAM-11 antibody); (C) ICAM-1; (D) VCAM-1; and (E) neutral lipid (oil red O [ORO]). (F) Lipid was extracted from each of the grafts, and total cholesterol content was measured with mass spectrometry. Data points are values for individual grafts; bars are group means \pm SEM. p values are from ANOVA, with correction for pairwise post hoc comparisons. (G–I) Representative sections of vein grafts harvested 12 weeks after vector infusion and stained with (G) HHF-35 antibody, (H) RAM-11 antibody, or (I) ORO. Dashed lines indicate internal elastic lamina. Scale bars, 500 μ m. Inset in (G) shows HHF-35-positive area in intima (arrow). M, media; I, intima. Scale bar, 200 μ m (see also Figures S3–S5).

30% lower ($p < 0.05$) at 8 weeks (Figure 7C). Graft lumen diameters and areas were similar between the 2 groups at both time points (Figures 7D and 7E). Percent lumen stenosis ($\sim 20\%$) was also similar between the DMEM and HDAdNull groups at both time points (Figure 7F).

Sections of the same 45 grafts were stained to detect intimal T cells, macrophages, and adhesion molecules. T cells were rare in intimas of DMEM-infused grafts at both time points. HDAdNull-infused grafts harvested at the 2-week time point had a trend toward more intimal area occupied by T cells (5.8-fold increase; $p = 0.09$; Figures 8A, S7A, and S7B). Intimas of HDAdNull-infused grafts harvested 8 weeks after infusion had significantly more T cell stained area than did DMEM-infused grafts (2.6-fold; $p < 0.01$; Figures 8A, S7D, and S7E). Rare macrophages were present in intimas of DMEM-infused grafts harvested 2 weeks after infusion, with a slight absolute increase

above this low level at 8 weeks. Compared to DMEM-infused grafts, HDAdNull-infused grafts had significantly increased intimal macrophage staining at 2 weeks (2.5-fold; $p = 0.046$; Figures 8B, S8A, and S8B), but not at 8 weeks (Figures 8B, S8D, and S8E). ICAM-1-positive intimal area was significantly increased in HDAdNull-infused grafts compared to DMEM-infused grafts at 2 weeks (3.4-fold; $p = 0.04$; Figures 8C, S9A, and S9B) but not at 8 weeks (Figures 8C, S9D, and S9E). Compared to DMEM-infused grafts, VCAM-1-stained intimal area

Vein Graft Morphometry, Inflammatory Cells, and Adhesion Molecules

We assessed morphometry in 45 vein grafts (tissue from 4 grafts was lost due to a processing error). A neointima was present in all grafts, with no significant differences between HDAdNull- and DMEM-infused grafts at both 2 and 8 weeks (Figures 7A and S6). Medial areas were also similar at both time points (Figure 7B). Intima/media area ratios of HDAdNull veins were similar to DMEM veins at 2 weeks and

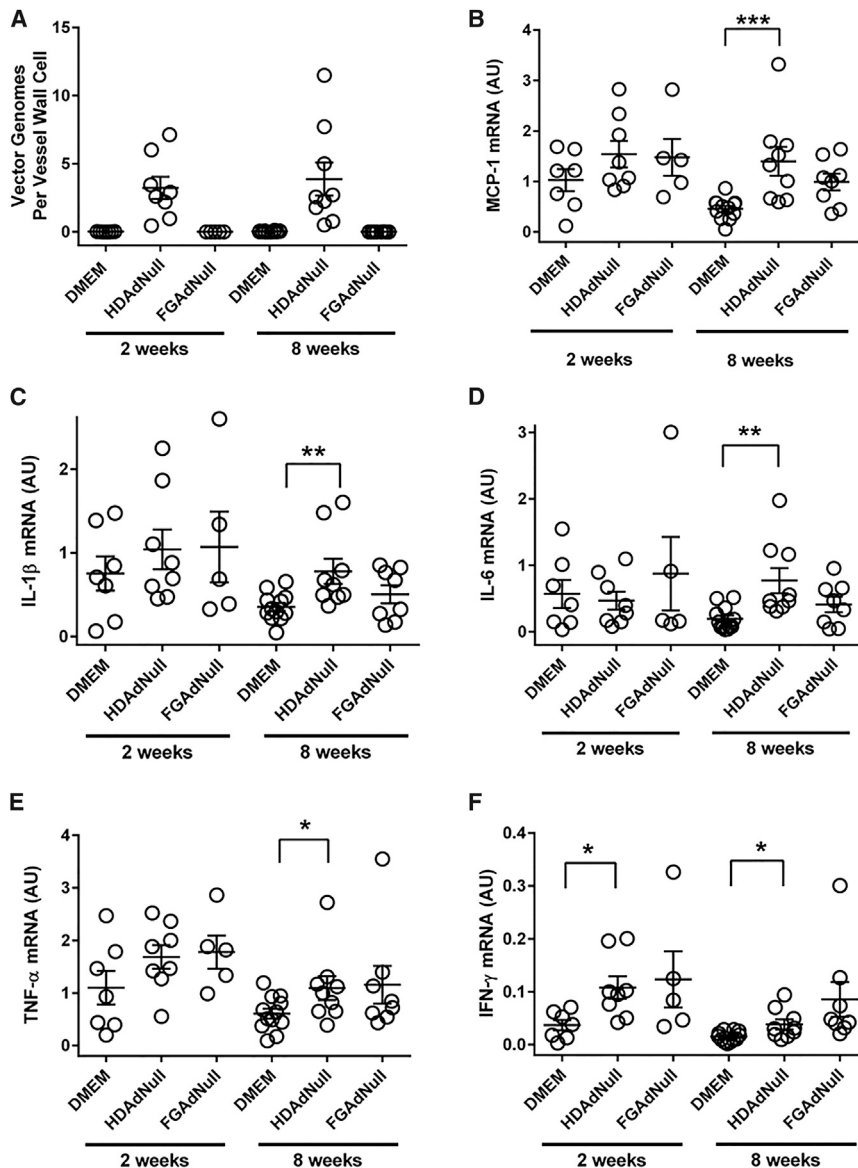


Figure 6. Vector Genomes and Inflammatory Cytokine Expression in Vein Grafts Harvested from Chow-Fed Rabbits

4 weeks after placement, grafts were infused with DMEM, HDAdNull, or FGAdNull and harvested 2 weeks ($n = 7, 8,$ and $5,$ respectively) or 8 weeks later ($n = 12, 9,$ and $8,$ respectively). (A) Vector DNA was measured by qPCR. (B–F) Levels of mRNA encoding (B) MCP-1, (C) IL-1 β , (D) IL-6, (E) TNF- α , and (F) IFN- γ were measured with qRT-mediated PCR, with normalization to GAPDH mRNA in the same samples. Data points are individual grafts; bars are group means \pm SEM. * $p < 0.05$; ** $p < 0.01$; *** $p < 0.001$. p values are from rank-sum tests.

larity, vector DNA, and cytokine as well as adhesion molecule expression. The study in chow-fed rabbits revealed that—compared to buffer infusion—HDAd infusion into grafted veins (1) moderately increases expression of inflammatory cytokines; (2) minimally increases accumulation of intimal T cells and transiently increases accumulation of intimal macrophages; (3) has variable effects on adhesion molecule expression; and (4) does not increase neointimal growth or lumen stenosis.

Our long-term goal is to increase patency of coronary artery bypass vein grafts. Because atherosclerosis is the most common cause of coronary artery bypass vein graft failure,¹² we sought to develop an animal model that replicates the key features of human vein graft atherosclerotic lesions: concentric intimal accumulation of lipid and macrophage-derived foam cells.^{12,48,49} A lipid and macrophage-rich vein graft intima is viewed as a pathological substrate that eventually leads to plaque rupture, superimposed thrombosis, and lumen occlusion.^{50,51} The likelihood that lipid and foam

in HDAdNull-infused grafts was similar at 2 weeks and significantly decreased at 8 weeks (55%; $p < 0.05$; Figures 8D and S10).

DISCUSSION

We developed a fat-fed rabbit model for testing HDAd-mediated gene therapy for vein graft atherosclerosis. In a separate study in chow-fed rabbits, we tested whether HDAd infusion into grafted veins causes inflammation and intimal growth. Our major findings in the atherosclerosis model are (1) vein grafts rapidly and consistently develop a large lipid- and macrophage-rich neointima; (2) outward remodeling prevents development of luminal stenosis; (3) HDAd genomes decline over time, although they remain at a high level through 20 weeks after gene transfer; and (4) our protocol allows use of single vein grafts to measure hemodynamics, wall morphology and cellu-

cell accumulation contributes importantly to vein graft failure is bolstered by the efficacy of lipid-lowering therapy in retarding vein graft atherosclerosis,^{14,15,52} as well as evidence that vein grafts are more prone to lipid accumulation than arteries.⁴⁸ Lesions in our model are rich in both lipid and macrophage-derived foam cells and are therefore a suitable substrate for testing atheroprotective vein graft gene therapy. Moreover, our protocols allow measurement of the critical variable of graft lipid accumulation with 2 independent approaches: oil red O staining and mass spectrometry. We acknowledge that—unlike coronary bypass grafts—human peripheral artery bypass grafts typically fail due to intimal hyperplasia rather than atherosclerosis.⁵³ Therefore, our atherosclerosis model does not address the most common cause of peripheral artery bypass graft failure.

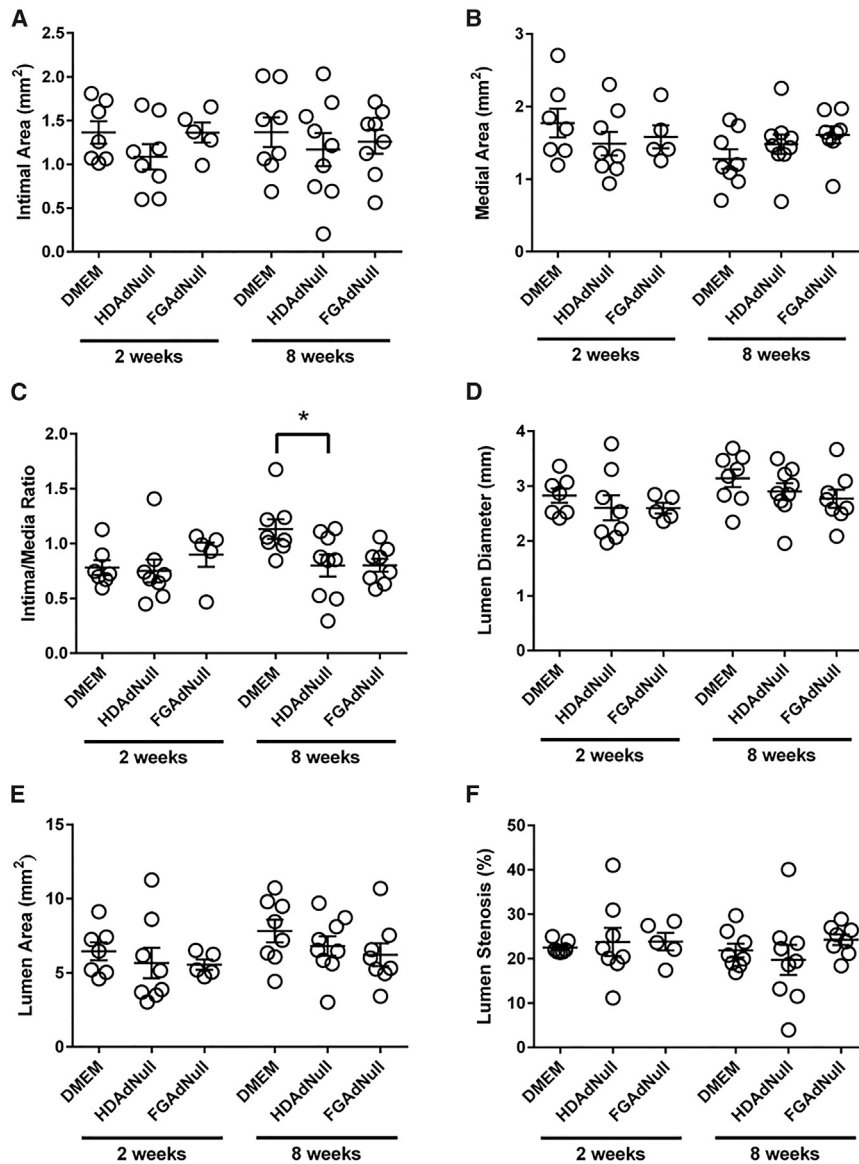


Figure 7. Morphometry of Vein Grafts Harvested from Chow-Fed Rabbits

4 weeks after placement, grafts were infused with DMEM, HDAdNull, or FGAdNull and harvested 2 weeks (n = 7, 8, and 5, respectively) or 8 weeks later (n = 8, 9, and 8, respectively). Three segments of each of the grafts were embedded, sectioned, and stained with Verhoeff van Gieson stain. Images of stained sections were analyzed with computer-assisted planimetry to determine (A) intimal area; (B) medial area; (C) intima/media area ratio; (D) lumen diameter; (E) lumen area; and (F) percent lumen stenosis. Data points are values for individual grafts; bars are group means ± SEM. *p < 0.05 (from t test) (see also Figure S6).

4 weeks. We believe that the decline in cytokine expression between 4 and 12 weeks is likely due to acute cytokine upregulation in 4-week grafts as a consequence of the recent surgery and vector infusion.⁵⁴ Because we are developing a therapy for vein graft atherosclerosis, rather than for surgery- and vector-related inflammation, 12 weeks again seems to be a better time point for experimental vein graft harvests.

To further assess the usefulness of this model, we used the 12-week group means and SDs for macrophage and lipid accumulation (i.e., RAM-11-stained area, oil-red-O-stained area, and total vein wall cholesterol measured with mass spectrometry) to calculate sample sizes needed for experiments that would test a gene therapy intervention. To detect or exclude a gene-therapy-related 30% difference in RAM-11-stained area, oil-red-O-stained area, and total vein wall cholesterol (with $\alpha = 0.05$ and $\beta = 0.2$), 11, 17, and 23 rabbits (each with 2 vein grafts) would be required, respectively. Accordingly, a study with 25 rabbits (only modestly larger than the present study and

To identify an optimal time point for detecting treatment effects in future experiments that test gene therapy interventions, we harvested veins at 3 intervals after vector infusion: 4, 12, and 20 weeks. In selecting an optimal time point, we looked for large increases in key pathologic end points (especially lipid and macrophage accumulation), relatively low intragroup variability (enabling use of smaller sample sizes), and a relatively short period of time after vector infusion (to minimize cost and increase experimental throughput). Based on these criteria, harvesting grafts 12 weeks after vector infusion appears optimal. Graft lipid content increases significantly between 4 and 12 weeks, but does not increase further between 12 and 20 weeks. Expression of ICAM-1 tends to increase between 4 and 12 weeks, whereas VCAM-1 is essentially unchanged. In contrast, expression of atherogenic cytokines was uniformly lower at 12 weeks than at

therefore feasible) would be powered to detect or exclude treatment-related reductions as low as 20%, 25%, and 29% in these same 3 end points. We plan to use this vein graft atherosclerosis model to test gene therapy that delivers apolipoprotein (apo) A-I from the luminal endothelium (Wacker et al., 2017, *Arterioscler. Thromb. Vasc. Biol.*, abstract).³³ It is logical to deliver apo A-I from the luminal endothelium because endogenous apo A-I enters the vessel wall from the vascular lumen via endothelial transcytosis.⁵⁵ Therefore, expression of apo A-I in the endothelium exploits the endogenous pathway for apo A-I entry to the blood vessel wall. Gene therapy strategies that envision gene delivery to medial or adventitial cells are also worthy of consideration. The media might be targeted by transgenes that prevent smooth muscle cell proliferation and migration and the adventitia could be targeted by transgenes that prevent migration of adventitial

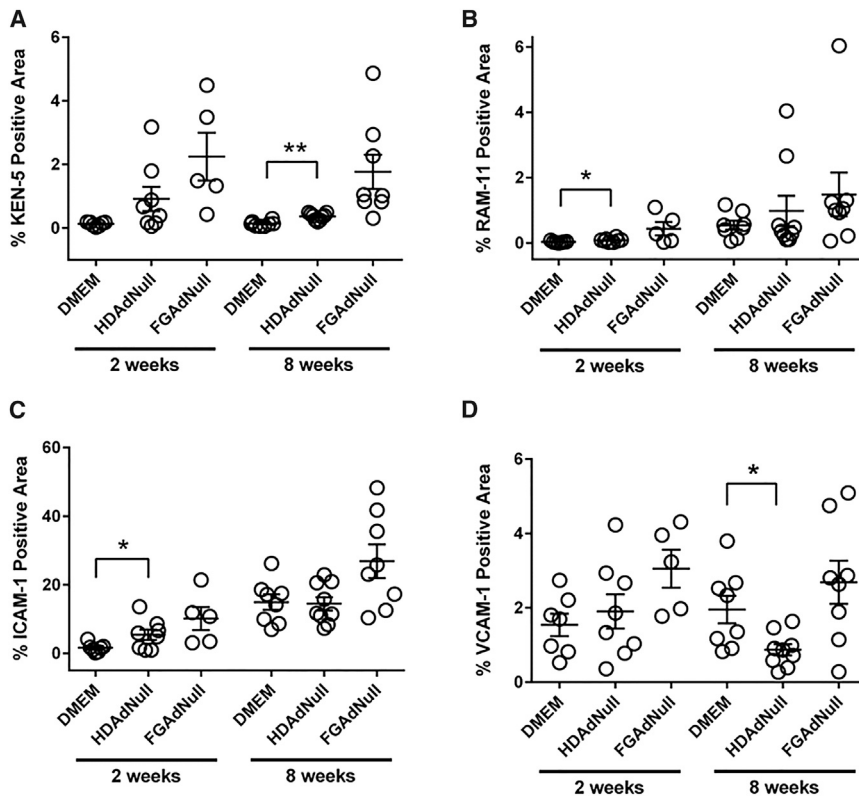


Figure 8. Cellularity and Adhesion Molecule Expression in Vein Grafts Harvested from Chow-Fed Rabbits

4 weeks after placement, grafts were infused with DMEM, HDAdNull, or FGAdNull and harvested 2 weeks (n = 7, 8, and 5, respectively) or 8 weeks later (n = 8, 9, and 8, respectively). Three segments of each of the grafts were embedded, sectioned, and stained with antibodies. Images of stained sections were analyzed with computer-assisted planimetry to determine the percentage of intimal area stained for (A) T cells (KEN-5 antibody); (B) macrophages (RAM-11 antibody); (C) ICAM-1; and (D) VCAM-1. Data points are mean values for individual grafts; bars are group means \pm SEM. * $p < 0.05$; ** $p < 0.01$. p values are from t tests (A–C) and rank-sum test (D) (see also Figures S7–S10).

cells into the intima. These strategies might be effective in preventing neointimal hyperplasia, which contributes to early CABG failure and is the principal cause of peripheral artery bypass graft failure.^{10,53} However, efficient transduction of the media and adventitia is technically challenging, whereas efficient gene transfer to endothelium can be achieved by intraluminal incubation of adenovirus.

Our model of vein graft atherosclerosis is promising, but it also has limitations. First, there is no development of stenosis because—at least through 20 weeks after transduction—outward remodeling compensates for intimal growth and prevents lumen loss. Outward remodeling was greater in vein grafts of hyperlipidemic rabbits than in chow-fed rabbits, potentially due to accumulation of macrophages in the vein graft wall and concomitantly higher levels of matrix metalloproteinases.⁵⁶ Nevertheless, because the vein grafts do not develop stenosis, we cannot use this model to test whether an intervention prevents vein graft stenosis. We assume, however, that an intervention that prevents lipid and macrophage accumulation would also prevent persistent intimal growth and eventual development of necrotic cores and vulnerable plaques that lead to vein graft stenosis and occlusion.^{12,51} Although this seems likely, we acknowledge that it is an assumption. We are not aware of any vein graft atherosclerosis animal models that develop hemodynamically significant stenoses, in which this could be tested.

Another limitation of this model is that transduction is performed 4 weeks after graft placement. We delayed transduction until 4 weeks

because our previous work showed that near-complete early (3 day) loss of vein-graft transgene expression could be avoided only by transducing grafted veins at a time point after the grafting surgery.²⁶ This earlier study was performed largely with FGAd, and we concede that we have not tested whether delivery of HDAd at the time of grafting would yield persistent transgene expression. However, we believe this is highly unlikely because our control experiments showed that loss of FGAd genomes within 3 days after grafting is due to exposure of the transduced veins to arterial flow and pressure, not to FGAd properties per se.²⁶

In the preclinical setting, a delay of 4 weeks between vein grafting and gene transfer is impractical but manageable. In the clinical setting, delayed transduction would likely require a catheter-based intervention to deliver the vector to the vein graft lumen, adding to the cost and potential complications associated with the therapy. This limitation might someday be overcome by development of vectors that home to the blood vessel wall after percutaneous injection.⁵⁷ Delaying transduction for 4 weeks also raises the possibility of missing a critical therapeutic window for delivering gene therapy that prevents occlusive vein graft disease. We cannot exclude this possibility, but we think it is unlikely. Vein graft atherosclerosis—the most common cause of coronary artery bypass vein graft occlusive disease—does not typically cause stenoses and occlusions until years after grafting.^{10,13,48} Delivery of gene therapy within 1 month of grafting would seem sufficiently early to forestall a process that does not become clinically manifest until much later. We are aware that the PREVENT IV study showed a surprisingly high incidence of early coronary artery bypass vein graft failure: 29% on a per-graft basis within 12–18 months.⁵⁸ These early failures are likely not due to vein graft atherosclerosis, which is a more indolent process. The possibility was raised by both the PREVENT investigators and others that this unexpectedly high rate of early failures might result from the technique used to

deliver the nucleic acid decoy.^{58,59} If so, this atypical early occlusion rate should not be encountered routinely.

A third potential limitation of our approach is lack of persistence of HDAd in atherosclerotic vein grafts. HDAd genomes in the vein grafts declined substantially between 4 and 20 weeks after transduction, although they remained at a relatively high absolute level (~4 vector genomes per endothelial cell). Genome loss during this interval may reflect disappearance of transcriptionally inactive genomes (as occurs between 3 and 28 days after transduction),⁵⁴ and loss of transcriptionally inactive genomes would not affect vector-derived transgene expression. Nevertheless, additional work is needed to determine whether HDAd can mediate long-lasting (i.e., years) transgene expression in atherosclerotic vein grafts.

Another potential limitation of our model is that the rabbits are severely hyperlipidemic, more so than virtually any human. Accordingly, they develop intimal lesions that—compared to many human saphenous vein graft lesions^{13,49}—are apparently richer in macrophages and lipid and poorer in smooth muscle cells. We were surprised by the small amount of intimal staining for muscle actin (~2% of intimal area). It is possible that this stain underestimates the percentage of intima that is occupied by cells of smooth muscle lineage because, as is well documented in mice and humans,⁶⁰ smooth-muscle-derived intimal cells are phenotypically modulated away from a contractile (i.e., muscle actin-expressing) phenotype. This hypothesis is supported by the faint intensity of muscle actin staining of vein graft intima compared to the intense medial staining of an ungrafted rabbit vein probed with the same antibody (Figure S3A). However, even if cells of smooth muscle lineage are minor contributors to intimal growth in this model, the model remains well suited for testing therapies that prevent lipid and macrophage accumulation.

We also tested whether infusion of HDAd in grafted veins has pro-inflammatory effects or promotes neointimal growth. Beginning several years ago, we investigated the pro-inflammatory effects of Ad vectors⁶¹ by infusing FGAd into arteries of chow-fed and fat-fed rabbits as well as fat-fed monkeys. In all 3 settings, FGAd increased arterial inflammation and either intimal area or cellularity.^{29,30,62} Others reported similar findings in arteries of chow-fed rabbits^{46,47} and in murine vein grafts.⁶³ In contrast, infusion of HDAd in arteries of either chow-fed or fat-fed rabbits (at 5×10^{11} to 7.5×10^{11} particles/mL) produced significantly less inflammation and intimal growth than did FGAd, but still more than buffer alone.^{28,29} Moreover, infusion of HDAd in fat-fed rabbits at a lower dose (2×10^{11} particles/mL, which achieves near-maximal transgene expression)^{27,64} did not significantly increase inflammation or intimal growth compared to buffer infusion.²⁹ Accordingly, we selected the 2×10^{11} particles/mL dose, and we used this dose in an earlier study in which we developed a rabbit vein graft transduction protocol.²⁶

In the present study, to assess the pro-inflammatory effects of HDAd in vein grafts, we also infused HDAd at 2×10^{11} particles/mL, we used

chow-fed rabbits, and we measured intimal area and inflammatory markers at 2 time points. We used a dose of 2×10^{11} particles/mL because this dose is effective in our arterial gene therapy models and achieves efficient gene transfer in rabbit vein grafts.^{26,27,33} We used chow-fed rabbits to decrease background intimal growth and inflammation that are caused (in arterial gene transfer models) by fat feeding and buffer infusion alone.^{29,32} With a lower background for these end points in vein grafts of chow-fed rabbits, we anticipated an increased sensitivity to detect HDAd-induced changes. We found that—in this model—HDAd did not promote intimal growth compared to buffer infusion; however, it had modest pro-inflammatory effects. These pro-inflammatory effects varied over time, with temporal variation that was inconsistent among cytokines, adhesion molecules, and inflammatory cells.

In summary, we developed a rabbit vein graft atherosclerosis model that will be useful for testing gene therapy interventions aimed at limiting lipid and macrophage accumulation in the vein graft intima. We also found that HDAd has pro-inflammatory effects in vein grafts of chow-fed rabbits, even when it is infused at the relatively low dose of 2×10^{11} particles/mL (a dose that does not significantly increase inflammation in arteries of fat-fed rabbits).²⁹ Whether these inflammatory effects will preclude use of HDAd for vein graft gene therapy and whether the pro-inflammatory effects might be decreased or eliminated either by expression of an anti-inflammatory cytokine such as IL-10⁵⁴ or by expression of a therapeutic transgene that has anti-inflammatory activity (e.g., apo A-I)^{33,65} will require further testing. We look forward to performing future studies that answer these questions and further clarify the potential of HDAd to deliver durable and effective gene therapy for vein graft atherosclerosis.

MATERIALS AND METHODS

Adenoviral Vectors

We used 2 adenoviral vectors: FGAdNull and HDAdNull. FGAdNull is a first-generation E1/E3-deleted adenoviral vector.⁶⁶ HDAdNull is a 3rd generation or “helper-dependent” adenoviral vector that lacks all viral genes.^{34,67} Both vectors contain the same empty expression cassette, including the cytomegalovirus immediate-early promoter and the SV40 polyadenylation signal, but no transgene. FGAdNull was amplified in 293 cells and HDAdNull in 293Cre4 cells,⁶⁸ both were purified by cesium chloride ultracentrifugation. Virion concentration was measured by spectrophotometry.⁶⁹ We used a single preparation of FGAdNull (6.0×10^{12} viral particles [vp]/mL). We used one preparation of HDAdNull (1.5×10^{12} vp/mL) for the vein-graft atherosclerosis study and a second preparation (1.0×10^{12} vp/mL) for the study in chow-fed rabbits aimed at determining whether HDAdNull causes vascular inflammation (hereafter termed the “inflammation” study). E1A copies in all preparations were <1 in 10^6 vector genomes, as measured by qPCR.³⁴ Both HDAdNull preparations had 1% helper virus contamination, determined by qPCR. Primers and probes are in Table S4. Both vectors were diluted with DMEM (Life Technologies, Grand Island, NY) before infusion. HDAdNull was infused at a concentration of 2×10^{11} vp/mL (the same concentration used in our gene therapy studies).^{27,33} Because FGAdNull was used only as a positive

control for detection of vector-related inflammation (in a study designed to compare HDAdNull and DMEM vehicle), it was infused at a higher concentration (7.5×10^{11} vp/mL).

Animals and Survival Surgeries

All animal studies were approved by the University of Washington Office of Animal Welfare. Specific pathogen-free adult male New Zealand White rabbits (3.0–3.5 kg) were purchased (Western Oregon Rabbit, Philomath, OR). After arrival, rabbits were acclimated to the animal facility for at least 1 week and fed regular chow (Albers 16% rabbit PLT, Pacific Northwest Milling, Bellevue, WA). Rabbits enrolled in the atherosclerosis model study were then switched to a high-fat diet, described below. Rabbits enrolled in the inflammation study were fed regular chow for the duration of the study. All rabbits were fed 150 g/day of chow. Diets and surgical protocols for the atherosclerosis model and inflammation studies are illustrated in Figure 1.

Eighteen rabbits were enrolled in the atherosclerosis model study and 15 completed the study. Two rabbits died from anesthesia complications during the gene transfer surgery and one was euthanized due to respiratory distress on postoperative day 2 after gene transfer. After these deaths, we modified our anesthesia protocol for vein graft gene-transfer surgeries to include intubation rather than mask ventilation and no deaths occurred after this change. Rabbits were enrolled in the atherosclerosis model study by initiation of a high-fat diet, including 0.3% cholesterol with 3% soybean oil (Dyets, Bethlehem, PA). Total plasma cholesterol was measured after 2 weeks of this diet and then every 2 weeks thereafter using a colorimetric assay (Abbott Laboratories, Abbott Park, IL). Based on these plasma cholesterol measurements, diets were adjusted (0.25%, 0.125%, or 0% cholesterol) to maintain plasma cholesterol within a range of 200–800 mg/dL. The 0.125% cholesterol diet was achieved by mixing the 0.25% cholesterol diet and regular chow at a 1:1 ratio.

Vein grafting was performed 4 weeks after beginning the high-fat diet. Grafting was performed under general anesthesia. Rabbits were sedated with intramuscular ketamine (30 mg/kg) and xylazine (3 mg/kg), and then maintained under anesthesia with inhaled isoflurane (1%–3%). Briefly, a 6-cm vertical incision was made in the neck midline, and approximately 3-cm lengths of both external jugular veins and both common carotid arteries were exposed by dissection of surrounding soft tissues and ligation of branches. After administration of intravenous heparin (150 U/kg), the right external jugular vein was ligated, excised, and placed as a reversed interposition graft in the adjacent common carotid artery. Vein-to-artery anastomoses were performed in an end-to-side manner using interrupted 7-0 polypropylene sutures. This procedure was repeated on the left side. 4 weeks after grafting, the rabbit was anesthetized and the neck was re-opened. The grafted veins were exposed via dissection and the right vein graft was isolated between vascular clips placed on the adjacent artery. An arteriotomy was performed caudal to the grafted vein, the vein lumen was rinsed out with DMEM, and the lumen was infused via the arteriotomy with HDAdNull. A silk tie was used to hold the

infusion cannula in place and prevent leakage via the arteriotomy. After 20 min incubation, the infusate was aspirated, the arteriotomy was repaired, and blood flow was restored. The procedure was repeated on the left side. Vein-graft patency was assessed by transcutaneous ultrasonography performed 5–7 days after placement of vein grafts and again 5–7 days after gene transfer surgery.

Twenty-nine rabbits were enrolled in the inflammation study and 26 completed the study. One rabbit had a febrile illness after vein grafting and was removed from the study. Another rabbit was found to have a subcutaneous neck abscess at the gene transfer surgery and was euthanized. A third rabbit died 3 hr post DMEM infusion due to general anesthesia complications. Surgical protocols for vein grafting and gene transfer were identical to those in the atherosclerosis model study except that vein grafts in the inflammation study were infused either with DMEM, HDAdNull, or FGAdNull. The same infusate was used in both vein grafts of an individual rabbit.

Transcutaneous Ultrasound

We used a SonoScape S8 portable color Doppler ultrasound instrument (Sonoscape, Shenzhen, China). For examinations of vein graft patency performed 5–7 days after surgery, non-anesthetized rabbits were wrapped in a blanket and held in a supine position. The rabbit's neck was extended, covered with ultrasound gel and examined with a 5–10 MHz probe (wavelengthMP, Jorgensen Laboratories, Loveland, CO). Vein grafts were considered to be patent if intraluminal pulsatile flow was visualized by Doppler exam. We also used transcutaneous ultrasound to measure vein graft internal diameters during the terminal surgeries. After achieving general anesthesia, before skin incision, the ultrasound probe was placed on the neck and the internal diameter of each graft was measured at 3 levels: within the caudal, medial, and cranial third.

In Vivo Flow Measurements

We measured blood flow in vein grafts with a 2-mm perivascular flow probe and a volume-flow meter (Model T402 Transonic Systems, Ithaca, NY), and recorded data with a PowerLab4/30 recording unit with LabChart software (ADInstruments, Colorado Springs CO). After exposure of vein grafts and adjacent carotid arteries, the surgical wound cavity was filled with physiological saline to enable transmission of sound waves. The flow probe (pre-sterilized with hydrogen peroxide gas plasma) was placed around the carotid artery adjacent to the vein graft. In most cases the probe was applied caudally to the graft. In the atherosclerosis model study, flow measurements were made only during the terminal surgery. In the inflammation study, flow measurements were also performed on several unoperated carotid arteries to determine baseline carotid blood flow under anesthesia. Blood flow in grafted veins was measured both during the vector infusion surgery (before vector infusion) and during the terminal surgery. The vein graft pulsatility index was calculated using the formula: pulsatility = (maximum blood flow rate – minimum blood flow rate)/mean blood flow rate. Shear stress (τ , dynes/cm²) was calculated using the formula: $\tau = 4\eta f/\pi r^3$. η (blood viscosity), 0.046 poise;⁷⁰ f , blood flow (mL/s); and r , radius of vein graft (cm).

Vein Graft Harvests

For the atherosclerosis model study, grafts were harvested 4, 12, or 20 weeks after vector infusion. For the inflammation study, grafts were harvested 2 or 8 weeks after infusion. Rabbits were anesthetized as described above, except that isoflurane was delivered via a mask. A midline incision was made and the vein grafts were exposed along with adjacent segments of the common carotid arteries. After measurement of blood flow with the volume flow meter, the grafts were isolated from the circulation with silk ligatures, excised, gently flushed with DMEM, and cut transversely into 5 equal segments (Figures S11A and S11B). Segments 1, 3, and 5 were embedded in optimal cutting temperature medium for frozen sectioning (Figure S11C). Segments 2 and 4 were divided axially to yield 2 segments each. These 4 segments were snap frozen in liquid nitrogen and stored at -80°C . For the atherosclerosis model study (Figure S11A), one half of both segment 2 and segment 4 were used to measure tissue lipids by mass spectrometry (see below). Extracts of the other halves of these two segments were used for DNA and RNA analyses. For the inflammation study (Figure S11B), one half of segment 2 and segment 4 were used for DNA analysis and the other halves were used for RNA analyses. A normal external jugular vein of a chow-fed rabbit in a separate study³⁴ was harvested during a terminal surgery and embedded into optimal cutting temperature medium for frozen sectioning.

Measurement of Viral Genomes

For the atherosclerosis model study, tubes containing the halves of segments 2 and 4 of each vein that were designated for DNA/RNA analyses (Figure S11A) were removed from -80°C storage and placed together in liquid nitrogen. The 2 segments were ground to a powder with a mortar and pestle that had been pre-cooled with liquid nitrogen. Approximately 1/3 of the powder was used for measurement of viral genomes. Total DNA was extracted from the powder with the DNeasy kit (QIAGEN Sciences, Germantown, MD) and quantified by spectrophotometer (NanoDrop; Thermo Scientific, Wilmington, DE). HDAdNull vector copy number was measured by quantitative real-time PCR amplification of 100 ng total DNA using primers targeting a sequence of noncoding stuffer DNA. FGAdNull vector DNA was measured similarly using primers targeting the CMV promoter. The sequences of primers and probes are listed in Table S4. For HDAdNull, copy number was calculated based on a standard curve prepared by serial dilution of the pC4HSU plasmid (Microbix Biosystems, Ontario, Canada), which contains the stuffer DNA sequence. For FGAdNull, the standard curve was prepared by serial dilution of the pCI plasmid (Promega, Madison, WI). Vector genomes per vascular wall cell were calculated by dividing the number of vector genomes detected in a well by the number of diploid cells represented by 100 ng DNA. For the inflammation study (Figure S11B), DNA was extracted from the combined halves of segments 2 and 4 with the DNeasy kit, without tissue grinding.

Measurement of mRNA

For the atherosclerosis model study, approximately 2/3 of the powder obtained by grinding the vein graft segments designated for DNA/

RNA analyses was used for mRNA measurements. Frozen vein segments were pulverized in liquid nitrogen and homogenized (Polytron Devices, Paterson, NJ) in the buffer from the RNeasy mini kit (QIAGEN Sciences, Germantown, MD), with 1% β -mercaptoethanol added. Total RNA was extracted with the RNeasy kit (QIAGEN Sciences, Germantown, MD), quantified by spectrophotometry (NanoDrop, Thermo Scientific, Wilmington, DE), and treated with DNase I (Thermo Scientific). For the inflammation study, we combined the halves of segments 2 and 4 that were not used for DNA extraction, pulverized them, and extracted RNA using the same methods used for veins from the atherosclerosis study. The levels of mRNA of TNF- α , IL-1 β , IFN- γ , IL-6, and MCP-1 were measured by qRT-mediated PCR amplification using 50 ng RNA as a template and were normalized to levels of glyceraldehyde 3-phosphate dehydrogenase (GAPDH) mRNA measured in the same samples. Sequences of primers and probes are in Table S4.

Measurement of Tissue Cholesterol

Vessel segments frozen in liquid nitrogen were pulverized with a liquid nitrogen-cooled mortar and pestle. Pulverized tissue (5–10 mg) was transferred to a fresh tube, in which we isolated lipids by Folch extraction.⁷¹ Briefly, 640 μL chloroform and internal standards (10 μg [d7]cholesterol and 10 μg 17:0-CE) were added to the tube, followed by 320 μL methanol. The samples were incubated at room temperature for 15 min with periodic vortexing. Saline (240 μL) was added to the tube, followed by vortexing. After centrifugation at $600 \times g$ for 2 min, the lower organics layer was removed to a new tube and evaporated under nitrogen. The sample was resuspended in 500 μL chloroform and stored at -20°C .

Cholesterol was analyzed by mass spectrometry using modification of previously published procedures.^{72,73} To aid in detection, free cholesterol in the samples was derivatized to cholesteryl acetate. To accomplish this, we brought 0.5 mg tissue extract up to a volume of 200 μL by the addition of chloroform. We added 50 μL acetyl chloride and incubated the samples under nitrogen at room temperature for 90 min. Samples were quantified by direct-infusion ESI-MS on an AB Sciex 4000 Q Trap linear ion trap quadrupole liquid chromatography-tandem mass spectrometry (LC-MS/MS) mass spectrometer with Analyst software. A 10- μL sample volume was injected in a solvent mixture of 0.1% ammonium hydroxide in methanol at a flow rate of 0.1 mL/min. Parameters were optimized for CE analysis in positive ion mode with the following settings: spray voltage = 4,500 V; heater gas = 10 psi; curtain gas = 10 psi; nebulizer gas = 50 psi; Turbo spray temperature = 350°C ; collision energy = 15 eV for cholesterol acetate; and collision energy = 19 eV for long-chain cholesteryl ester (CE). Cholesterol and CE species were monitored by selective reaction monitoring using mass transition from the parent ion to cholestane (Table S5). Data were acquired for 1.2 min (quantification from 0.23 min when sample reaches the mass spectrometer until the end of data acquisition). Cholesterol signal was normalized to the [d7] cholesterol internal standard, whereas CE signal was normalized to the 17:0-CE internal standard. The signal from the long-chain CEs was further normalized by the response factors determined by

Liebisch et al.⁷³ for CE ammonium adducts to account for variations in ionization based on CE chain length and saturation (Table S5). The analyzed CE species were combined to determine total CE content. Quantitated masses of cholesterol and CE were normalized to the mass of extracted tissue. The final data represents the mean of two independent measurements for each vein graft (i.e., two separate samplings of the pulverized tissue, each of which were individually derivatized and measured by mass spectrometry).

Histochemical and Immunohistochemical Staining

The blocks of optimal cutting temperature medium (each containing 3 segments of a vein graft; Figures S11A and S11B) were sectioned at 2 steps, separated by 200 μm . At the first of these steps, 10 serial sections (6- μm thick) were cut and placed on different slides. At the next step, 10 serial sections were again cut and these sections were placed on slides, in order, adjacent to the sections cut at the first step. In this manner, each slide had 6 sections: 2 each from segments 1, 3, and 5, with the 2 sections of each segment separated by 200 μm (Figure S11C). Slides with these serial sections were stained with H&E, Verhoeff-Van Gieson (VVG), oil red O, and antibodies that detect rabbit macrophages (RAM-11; 1:1,000 dilution; Dako, Carpinteria, CA),⁷⁴ T cells (KEN-5; 1:50 dilution; Santa Cruz Biotechnology, Dallas, TX),⁷⁵ muscle actin (HHF-35; 1:200 dilution; Thermo Fisher Scientific, Waltham, MA),⁷⁶ VCAM-1 (Rb 1/9; 1:50 dilution), and ICAM-1 (Rb 2/3; 1:200 dilution).⁷⁷ The ICAM-1 and VCAM-1 antibodies were generous gifts from Dr. M. I. Cybulsky, University of Toronto. Sensitivity and specificity of the primary antibodies were ensured by use of positive controls (sections of blood vessels from previous experiments, known to stain positive) and negative controls (omission of the primary antibody). The secondary antibody was biotinylated goat anti-mouse immunoglobulin G (IgG) (1:200 dilution, Vector Laboratories, Burlingame, CA). Stained sections were photographed with a Leica DFC295 image system (Leica Microsystems, Buffalo Grove, IL) and evaluated with imaging analysis software (ImagePro Premier, Bethesda, MD) by observers blinded to the treatment group.

Intimal area, medial area, and perimeter of the internal elastic lamina (IEL) were measured directly on VVG-stained sections using computer-assisted planimetry; luminal areas and diameters were calculated. These measurements were made by observers blinded to treatment group. We used VVG-stained sections for these measurements because elastin (including the IEL as well as other medial elastic fibers) was most evident when stained with VVG. In these sections, we located the IEL and identified the most external (abluminal) medial elastic fibers that ran parallel to the IEL. We identified the intimal/medial border based on location of the IEL (typically fragmented) and the generally more intense staining of intimal versus medial tissue with the VVG stain (Figure S12A). We identified the medial/adventitial border based on the location of the most abluminal elastin fragments that ran parallel to the IEL as well as the more reticular structure of the adventitia versus the media (Figure S12). Elastin fragments at the medial/adventitial border were less easily identified than fragments of IEL. Therefore, we often used fluorescence micro-

scopy (with fluorescein wavelengths used to illuminate adjacent H&E-stained slides) to help locate the most abluminal medial elastin fragments (elastin is autofluorescent when illuminated with fluorescein wavelengths; Figures S12B and S12D). We calculated the area inside the IEL by measuring the IEL circumference and using the formula $\text{area} = \text{circumference}^2/4\pi$ (assumes circular geometry in vivo). Luminal areas were calculated by subtracting the intimal area from the area inside the IEL. Graft lumen diameters were calculated using the formula $\text{diameter} = \sqrt{4 \times \text{lumen area}/\pi}$. Percent luminal stenosis was calculated by dividing intimal area by the area inside the IEL. Measurements were made on multiple sections per vein graft (typically 4–6), omitting sections that were distorted by sectioning artifacts. For ~80% of the vein grafts, we acquired data from at least one section of each of the 3 segments.

To identify the intima on oil-red-O-stained sections, we used an adjacent VVG-stained section to trace the lumen and IEL. An image of this ring-like area was recorded using ImagePro, then superimposed on the adjacent oil-red-O-stained section and rotated as needed to achieve optimal overlap of the lumen contours of the image and the oil-red-O-stained section. The oil-red-O-stained intimal area was then measured using color thresholding. For the other stains, the IEL was sufficiently evident that intimal area could be measured on the same sections on which stained intimal area was quantified.

To assess reproducibility of the image analysis data for each of the stains, 2 to 3 observers independently analyzed 6–10 sections, measured intimal area, selected thresholds as needed for identifying the stained area, measured total stained intimal area, and calculated percent stained area. The observers then compared results, aiming for relative inter-observer differences of <10% (i.e., <2% absolute inter-observer differences for measured values of 20%–30% and 0.05% absolute inter-observer differences for measured values of 0.5%–1%). If larger differences were encountered for individual samples, the observers compared their technical approaches to improve consistency and the measurements were repeated until inter-observer differences were in the targeted range. We used a similar approach to evaluate reproducibility of the perimeter measurements made at the intimal/medial and medial/adventitial borders. This approach consisted of comparing the perimeter measurements obtained by 2 observers, discussing cases in which relative inter-observer differences exceeded 10%, and agreeing on an optimal technical approach in these cases. To evaluate inter-observer reproducibility for percent stained areas as well as perimeter lengths, the final measurements made by the observers were plotted against each other. These plots showed high correlations (typical $r^2 > 0.85$) and excellent agreement (typical slope of 0.9–1.1), consistent with high reproducibility.

We used H&E-stained sections from the atherosclerosis study to determine the ratio of endothelial cells to total vascular cells. For each section, we first counted luminal nuclei and then used the color-thresholding feature of the image-analysis program to count total nuclei in the section. The false-color images were examined and any nuclei not identified by the color-thresholding function were counted

manually. We performed this procedure on 4 sections from each of 12 veins, including 4 veins from each of the 4-, 12-, and 20-week harvests. We counted cells in 2 of the 4 quadrants of each section. Results were similar at all 3 time points and therefore were pooled.

Statistical Analyses

Data are presented as mean \pm SD, unless indicated otherwise. When 2 groups were compared, as in the inflammation study (in which the a priori hypothesis involved only the DMEM and HDAdNull groups, with the FGAdNull group included only as a positive control), the t test was used for normally distributed data with equal variances. The Mann-Whitney rank-sum test was used for comparing groups with either non-normally distributed data or unequal variances. For comparing more than two groups (as in the atherosclerosis study, in which results at 3 time points were compared), we used one-way ANOVA, with correction for post hoc pairwise comparisons with the Holm-Sidak method when data were normally distributed with equal variances. We used Kruskal-Wallis ANOVA when these conditions were not met. To evaluate inter-observer reproducibility, a scatterplot was used, and the slope of the regression line and the Pearson correlation coefficient were calculated to determine the relationship between 2 observers' measurements. Sample size calculations and statistical tests were performed with the SigmaStat program (Systat, San Jose, CA).

SUPPLEMENTAL INFORMATION

Supplemental Information includes twelve figures and five tables and can be found with this article online at <https://doi.org/10.1016/j.omtm.2017.09.004>.

AUTHOR CONTRIBUTIONS

Conceptualization, D.A.D.; Methodology, D.A.D., L.B., B.K.W., E.B., E.H.; Validation, D.A.D., L.B., B.K.W., E.B., E.H.; Formal Analysis, L.B., B.K.W., E.B., E.H.; Investigation, L.B., B.K.W., E.B., E.H., N.D.; Resources, N.D.; Data Curation, L.B., E.B., E.H., Writing – Original Draft, D.A.D., L.B., B.K.W., Writing – Review and Editing, D.A.D., L.B., B.K.W., E.B., E.H., N.D.; Visualization, D.A.D., L.B., B.K.W., E.B., E.H.; Supervision, D.A.D., L.B., B.K.W.; Project Administration, D.A.D., B.K.W.; Funding Acquisition, D.A.D.

CONFLICTS OF INTEREST

The authors declare no competing financial interests.

ACKNOWLEDGMENTS

We thank AdVec for permission to use HDAd-related materials, the Department of Comparative Medicine for invaluable assistance and support, Ms. Jingwan Zhang for excellent technical assistance, Dr. Eric Feigl for advice regarding hemodynamic measurements, Dr. Ted Kohler for advice on vein graft surgical technique, Dr. Burkhard Mackensen for advice on optimizing intraoperative anesthesia, and Ms. Julia Feyk for administrative assistance. This work was supported by a grant from the NIH (R01HL114541) and the John L. Locke Jr. Charitable Trust.

REFERENCES

1. National Center for Health Statistics. (2015). Health, United States, 2015: with special feature on racial and ethnic health disparities. <https://www.ncbi.nlm.nih.gov/books/NBK367640/>.
2. Roth, G.A., Huffman, M.D., Moran, A.E., Feigin, V., Mensah, G.A., Naghavi, M., and Murray, C.J. (2015). Global and regional patterns in cardiovascular mortality from 1990 to 2013. *Circulation* 132, 1667–1678.
3. Libby, P., Bornfeldt, K.E., and Tall, A.R. (2016). Atherosclerosis: successes, surprises, and future challenges. *Circ. Res.* 118, 531–534.
4. Libby, P. (2012). The vascular biology of atherosclerosis. In *Braunwald's Heart Disease: A Textbook of Cardiovascular Medicine*, Ninth Edition, R. Bonow, D.L. Mann, D.P. Zipes, and P. Libby, eds. (Elsevier Saunders), pp. 897–913.
5. Mohr, F.W., Morice, M.C., Kappetein, A.P., Feldman, T.E., Stähle, E., Colombo, A., Mack, M.J., Holmes, D.R., Jr., Morel, M.A., Van Dyck, N., et al. (2013). Coronary artery bypass graft surgery versus percutaneous coronary intervention in patients with three-vessel disease and left main coronary disease: 5-year follow-up of the randomised, clinical SYNTAX trial. *Lancet* 381, 629–638.
6. Velazquez, E.J., Lee, K.L., Jones, R.H., Al-Khalidi, H.R., Hill, J.A., Panza, J.A., Michler, R.E., Bonow, R.O., Doenst, T., Petrie, M.C., et al.; STICHES Investigators (2016). Coronary-artery bypass surgery in patients with ischemic cardiomyopathy. *N. Engl. J. Med.* 374, 1511–1520.
7. Chang, M., Ahn, J.M., Lee, C.W., Cavalcante, R., Sotomi, Y., Onuma, Y., Tenekcioglu, E., Han, M., Park, D.W., Kang, S.J., et al. (2016). Long-term mortality after coronary revascularization in nondiabetic patients with multivessel disease. *J. Am. Coll. Cardiol.* 68, 29–36.
8. Alexander, J.H., and Smith, P.K. (2016). Coronary-artery bypass grafting. *N. Engl. J. Med.* 374, 1954–1964.
9. Lopes, R.D., Mehta, R.H., Hafley, G.E., Williams, J.B., Mack, M.J., Peterson, E.D., Allen, K.B., Harrington, R.A., Gibson, C.M., Califf, R.M., et al.; Project of Ex Vivo Vein Graft Engineering via Transfection IV (PREVENT IV) Investigators (2012). Relationship between vein graft failure and subsequent clinical outcomes after coronary artery bypass surgery. *Circulation* 125, 749–756.
10. Harskamp, R.E., Lopes, R.D., Baisden, C.E., de Winter, R.J., and Alexander, J.H. (2013). Saphenous vein graft failure after coronary artery bypass surgery: pathophysiology, management, and future directions. *Ann. Surg.* 257, 824–833.
11. Sabik, J.F., 3rd (2011). Understanding saphenous vein graft patency. *Circulation* 124, 273–275.
12. Sarjeant, J.M., and Rabinovitch, M. (2002). Understanding and treating vein graft atherosclerosis. *Cardiovasc. Pathol.* 11, 263–271.
13. Cox, J.L., Chiasson, D.A., and Gotlieb, A.I. (1991). Stranger in a strange land: the pathogenesis of saphenous vein graft stenosis with emphasis on structural and functional differences between veins and arteries. *Prog. Cardiovasc. Dis.* 34, 45–68.
14. Post Coronary Artery Bypass Graft Trial Investigators (1997). The effect of aggressive lowering of low-density lipoprotein cholesterol levels and low-dose anticoagulation on obstructive changes in saphenous-vein coronary-artery bypass grafts. *N. Engl. J. Med.* 336, 153–162.
15. Kang, S., Liu, Y., and Liu, X.B. (2013). Effects of aggressive statin therapy on patients with coronary saphenous vein bypass grafts: a systematic review and meta-analysis of randomized, controlled trials. *Clin. Ther.* 35, 1125–1136.
16. Mehta, R.H., Ferguson, T.B., Lopes, R.D., Hafley, G.E., Mack, M.J., Kouchoukos, N.T., Gibson, C.M., Harrington, R.A., Califf, R.M., Peterson, E.D., et al.; Project of Ex-Vivo Vein Graft Engineering via Transfection (PREVENT) IV Investigators (2011). Saphenous vein grafts with multiple versus single distal targets in patients undergoing coronary artery bypass surgery: one-year graft failure and five-year outcomes from the Project of Ex-Vivo Vein Graft Engineering via Transfection (PREVENT) IV trial. *Circulation* 124, 280–288.
17. Kulik, A., Voisine, P., Mathieu, P., Masters, R.G., Mesana, T.G., Le May, M.R., and Ruel, M. (2011). Statin therapy and saphenous vein graft disease after coronary bypass surgery: analysis from the CASCADE randomized trial. *Ann. Thorac. Surg.* 92, 1284–1290.
18. Tatoulis, J., Buxton, B.F., and Fuller, J.A. (2004). Patencies of 2127 arterial to coronary conduits over 15 years. *Ann. Thorac. Surg.* 77, 93–101.

19. Taggart, D.P., Altman, D.G., Gray, A.M., Lees, B., Gerry, S., Benedetto, U., and Flather, M.; ART Investigators (2016). Randomized trial of bilateral versus single internal-thoracic-artery grafts. *N. Engl. J. Med.* *375*, 2540–2549.
20. Goldman, S., Sethi, G.K., Holman, W., Thai, H., McFalls, E., Ward, H.B., Kelly, R.F., Rhenman, B., Tobler, G.H., Bakaeen, F.G., et al. (2011). Radial artery grafts vs saphenous vein grafts in coronary artery bypass surgery: a randomized trial. *JAMA* *305*, 167–174.
21. Petrovic, I., Nezic, D., Peric, M., Milojevic, P., Djokic, O., Kosevic, D., Tasic, N., Djukanovic, B., and Otasevic, P. (2015). Radial artery vs saphenous vein graft used as the second conduit for surgical myocardial revascularization: long-term clinical follow-up. *J. Cardiothorac. Surg.* *10*, 127.
22. Bradshaw, A.C., and Baker, A.H. (2013). Gene therapy for cardiovascular disease: perspectives and potential. *Vascul. Pharmacol.* *58*, 174–181.
23. Southerland, K.W., Frazier, S.B., Bowles, D.E., Milano, C.A., and Kontos, C.D. (2013). Gene therapy for the prevention of vein graft disease. *Transl. Res.* *161*, 321–338.
24. Ylä-Herttua, S., and Baker, A.H. (2017). Cardiovascular gene therapy: past, present, and future. *Mol. Ther.* *25*, 1095–1106.
25. Ehsan, A., Mann, M.J., Dell'Acqua, G., and Dzau, V.J. (2001). Long-term stabilization of vein graft wall architecture and prolonged resistance to experimental atherosclerosis after E2F decoy oligonucleotide gene therapy. *J. Thorac. Cardiovasc. Surg.* *121*, 714–722.
26. Du, L., Zhang, J., Clowes, A.W., and Dichek, D.A. (2015). Efficient gene transfer and durable transgene expression in grafted rabbit veins. *Hum. Gene Ther.* *26*, 47–58.
27. Flynn, R., Qian, K., Tang, C., Dronadula, N., Buckler, J.M., Jiang, B., Wen, S., Dichek, H.L., and Dichek, D.A. (2011). Expression of apolipoprotein A-I in rabbit carotid endothelium protects against atherosclerosis. *Mol. Ther.* *19*, 1833–1841.
28. Wen, S., Graf, S., Massey, P.G., and Dichek, D.A. (2004). Improved vascular gene transfer with a helper-dependent adenoviral vector. *Circulation* *110*, 1484–1491.
29. Jiang, B., Qian, K., Du, L., Luttrell, I., Chitale, K., and Dichek, D.A. (2011). Helper-dependent adenovirus is superior to first-generation adenovirus for expressing transgenes in atherosclerosis-prone arteries. *Arterioscler. Thromb. Vasc. Biol.* *31*, 1317–1325.
30. Newman, K.D., Dunn, P.F., Owens, J.W., Schulick, A.H., Virmani, R., Sukhova, G., Libby, P., and Dichek, D.A. (1995). Adenovirus-mediated gene transfer into normal rabbit arteries results in prolonged vascular cell activation, inflammation, and neointimal hyperplasia. *J. Clin. Invest.* *96*, 2955–2965.
31. Zwolak, R.M., Kirkman, T.R., and Clowes, A.W. (1989). Atherosclerosis in rabbit vein grafts. *Arteriosclerosis* *9*, 374–379.
32. Du, L., Zhang, J., De Meyer, G.R., Flynn, R., and Dichek, D.A. (2014). Improved animal models for testing gene therapy for atherosclerosis. *Hum. Gene Ther. Methods* *25*, 106–114.
33. Wacker, B.K., Dronadula, N., Zhang, J., and Dichek, D.A. (2017). Local vascular gene therapy with apolipoprotein A-I to promote regression of atherosclerosis. *Arterioscler. Thromb. Vasc. Biol.* *37*, 316–327.
34. Flynn, R., Buckler, J.M., Tang, C., Kim, F., and Dichek, D.A. (2010). Helper-dependent adenoviral vectors are superior in vitro to first-generation vectors for endothelial cell-targeted gene therapy. *Mol. Ther.* *18*, 2121–2129.
35. Li, M., Tan, Y., Stenmark, K.R., and Tan, W. (2013). High pulsatility flow induces acute endothelial inflammation through overpolarizing cells to activate NF- κ B. *Cardiovasc. Eng. Technol.* *4*, 26–38.
36. Baeyens, N., Bandyopadhyay, C., Coon, B.G., Yun, S., and Schwartz, M.A. (2016). Endothelial fluid shear stress sensing in vascular health and disease. *J. Clin. Invest.* *126*, 821–828.
37. Meyerson, S.L., Skelly, C.L., Curi, M.A., Shakur, U.M., Vosicky, J.E., Glagov, S., Schwartz, L.B., Christen, T., and Gabbiani, G. (2001). The effects of extremely low shear stress on cellular proliferation and neointimal thickening in the failing bypass graft. *J. Vasc. Surg.* *34*, 90–97.
38. Channon, K.M., Fulton, G.J., Gray, J.L., Annex, B.H., Shetty, G.A., Blazing, M.A., Peters, K.G., Hagen, P.O., and George, S.E. (1997). Efficient adenoviral gene transfer to early venous bypass grafts: comparison with native vessels. *Cardiovasc. Res.* *35*, 505–513.
39. Schwartz, L.B., Moawad, J., Svensson, E.C., Tufts, R.L., Meyerson, S.L., Baunoch, D., and Leiden, J.M. (1999). Adenoviral-mediated gene transfer of a constitutively active form of the retinoblastoma gene product attenuates neointimal thickening in experimental vein grafts. *J. Vasc. Surg.* *29*, 874–881.
40. Eslami, M.H., Gangadharan, S.P., Sui, X., Rhynhart, K.K., Snyder, R.O., and Conte, M.S. (2000). Gene delivery to in situ veins: differential effects of adenovirus and adeno-associated viral vectors. *J. Vasc. Surg.* *31*, 1149–1159.
41. Chiu-Pinheiro, C.K., O'Brien, T., Katusic, Z.S., Bonilla, L.F., Hamner, C.E., and Schaff, H.V. (2002). Gene transfer to coronary artery bypass conduits. *Ann. Thorac. Surg.* *74*, 1161–1166.
42. Huynh, T.T., Iaccarino, G., Davies, M.G., Svendsen, E., Koch, W.J., and Hagen, P.O. (1998). Adenoviral-mediated inhibition of G beta gamma signaling limits the hyperplastic response in experimental vein grafts. *Surgery* *124*, 177–186.
43. Kibbe, M.R., Tzeng, E., Gleixner, S.L., Watkins, S.C., Kovacs, I., Lizonova, A., Makaroun, M.S., Billiar, T.R., and Rhee, R.Y. (2001). Adenovirus-mediated gene transfer of human inducible nitric oxide synthase in porcine vein grafts inhibits intimal hyperplasia. *J. Vasc. Surg.* *34*, 156–165.
44. Petrofski, J.A., Hata, J.A., Gehrig, T.R., Hanish, S.I., Williams, M.L., Thompson, R.B., Parsa, C.J., Koch, W.J., and Milano, C.A. (2004). Gene delivery to aortocoronary saphenous vein grafts in a large animal model of intimal hyperplasia. *J. Thorac. Cardiovasc. Surg.* *127*, 27–33.
45. Ross, R. (1999). Atherosclerosis—an inflammatory disease. *N. Engl. J. Med.* *340*, 115–126.
46. Channon, K.M., Qian, H.S., Youngblood, S.A., Olmez, E., Shetty, G.A., Neploueva, V., Blazing, M.A., and George, S.E. (1998). Acute host-mediated endothelial injury after adenoviral gene transfer in normal rabbit arteries: impact on transgene expression and endothelial function. *Circ. Res.* *82*, 1253–1262.
47. Gruchała, M., Bhardwaj, S., Pajusola, K., Roy, H., Rissanen, T.T., Kokina, I., Kholová, I., Markkanen, J.E., Rutanen, J., Heikura, T., et al. (2004). Gene transfer into rabbit arteries with adeno-associated virus and adenovirus vectors. *J. Gene Med.* *6*, 545–554.
48. Motwani, J.G., and Topol, E.J. (1998). Aortocoronary saphenous vein graft disease: pathogenesis, predisposition, and prevention. *Circulation* *97*, 916–931.
49. Nwasokwa, O.N. (1995). Coronary artery bypass graft disease. *Ann. Intern. Med.* *123*, 528–545.
50. Qiao, J.H., Walts, A.E., and Fishbein, M.C. (1991). The severity of atherosclerosis at sites of plaque rupture with occlusive thrombosis in saphenous vein coronary artery bypass grafts. *Am. Heart J.* *122*, 955–958.
51. Yazdani, S.K., Farb, A., Nakano, M., Vorpahl, M., Ladich, E., Finn, A.V., Kolodgie, F.D., and Virmani, R. (2012). Pathology of drug-eluting versus bare-metal stents in saphenous vein bypass graft lesions. *JACC Cardiovasc. Interv.* *5*, 666–674.
52. Blankenhorn, D.H., Nessim, S.A., Johnson, R.L., Sanmarco, M.E., Azen, S.P., and Cashin-Hemphill, L. (1987). Beneficial effects of combined colestipol-niacin therapy on coronary atherosclerosis and coronary venous bypass grafts. *JAMA* *257*, 3233–3240.
53. de Vries, M.R., Simons, K.H., Jukema, J.W., Braun, J., and Quax, P.H. (2016). Vein graft failure: from pathophysiology to clinical outcomes. *Nat. Rev. Cardiol.* *13*, 451–470.
54. Dronadula, N., Wacker, B.K., Van Der Kwast, R., Zhang, J., and Dichek, D.A. (2017). Stable in vivo transgene expression in endothelial cells with helper-dependent adenovirus: roles of promoter and interleukin-10. *Hum. Gene Ther.* *28*, 255–270.
55. Rohrer, L., Cavelier, C., Fuchs, S., Schlüter, M.A., Völker, W., and von Eckardstein, A. (2006). Binding, internalization and transport of apolipoprotein A-I by vascular endothelial cells. *Biochim. Biophys. Acta* *1761*, 186–194.
56. de Nooijer, R., Verkleij, C.J., van der Thüsen, J.H., Jukema, J.W., van der Wall, E.E., van Berkel, T.J., Baker, A.H., and Biessen, E.A. (2006). Lesional overexpression of matrix metalloproteinase-9 promotes intraplaque hemorrhage in advanced lesions but not at earlier stages of atherogenesis. *Arterioscler. Thromb. Vasc. Biol.* *26*, 340–346.
57. Van-Assche, T., Huygelen, V., Crabtree, M.J., and Antoniades, C. (2013). Gene delivery strategies targeting stable atheromatous plaque. *Curr. Pharm. Des.* *19*, 1626–1637.
58. Alexander, J.H., Hafley, G., Harrington, R.A., Peterson, E.D., Ferguson, T.B., Jr., Lorenz, T.J., Goyal, A., Gibson, M., Mack, M.J., Gennevois, D., et al.; PREVENT IV Investigators (2005). Efficacy and safety of edifoligide, an E2F transcription factor

- decoy, for prevention of vein graft failure following coronary artery bypass graft surgery: PREVENT IV: a randomized controlled trial. *JAMA* 294, 2446–2454.
59. Conti, V.R., and Hunter, G.C. (2005). Gene therapy and vein graft patency in coronary artery bypass graft surgery. *JAMA* 294, 2495–2497.
 60. Shankman, L.S., Gomez, D., Cherepanova, O.A., Salmon, M., Alencar, G.F., Haskins, R.M., Swiatlowska, P., Newman, A.A., Greene, E.S., Straub, A.C., et al. (2015). KLF4-dependent phenotypic modulation of smooth muscle cells has a key role in atherosclerotic plaque pathogenesis. *Nat. Med.* 21, 628–637.
 61. Kay, M.A., Glorioso, J.C., and Naldini, L. (2001). Viral vectors for gene therapy: the art of turning infectious agents into vehicles of therapeutics. *Nat. Med.* 7, 33–40.
 62. Schneider, D.B., Fly, C.A., Dichek, D.A., and Geary, R.L. (1998). Adenoviral gene transfer in arteries of hypercholesterolemic nonhuman primates. *Hum. Gene Ther.* 9, 815–821.
 63. Hu, Y., Baker, A.H., Zou, Y., Newby, A.C., and Xu, Q. (2001). Local gene transfer of tissue inhibitor of metalloproteinase-2 influences vein graft remodeling in a mouse model. *Arterioscler. Thromb. Vasc. Biol.* 21, 1275–1280.
 64. Du, L., Dronadula, N., Tanaka, S., and Dichek, D.A. (2011). Helper-dependent adenoviral vector achieves prolonged, stable expression of interleukin-10 in rabbit carotid arteries but does not limit early atherogenesis. *Hum. Gene Ther.* 22, 959–968.
 65. Rye, K.A., and Barter, P.J. (2008). Antiinflammatory actions of HDL: a new insight. *Arterioscler. Thromb. Vasc. Biol.* 28, 1890–1891.
 66. Falkenberg, M., Tom, C., DeYoung, M.B., Wen, S., Linnemann, R., and Dichek, D.A. (2002). Increased expression of urokinase during atherosclerotic lesion development causes arterial constriction and lumen loss, and accelerates lesion growth. *Proc. Natl. Acad. Sci. USA* 99, 10665–10670.
 67. Parks, R.J., Chen, L., Anton, M., Sankar, U., Rudnicki, M.A., and Graham, F.L. (1996). A helper-dependent adenovirus vector system: removal of helper virus by Cre-mediated excision of the viral packaging signal. *Proc. Natl. Acad. Sci. USA* 93, 13565–13570.
 68. Chen, L., Anton, M., and Graham, F.L. (1996). Production and characterization of human 293 cell lines expressing the site-specific recombinase Cre. *Somat. Cell Mol. Genet.* 22, 477–488.
 69. Mittereder, N., March, K.L., and Trapnell, B.C. (1996). Evaluation of the concentration and bioactivity of adenovirus vectors for gene therapy. *J. Virol.* 70, 7498–7509.
 70. Windberger, U., Bartholovitsch, A., Plasenzotti, R., Korak, K.J., and Heinze, G. (2003). Whole blood viscosity, plasma viscosity and erythrocyte aggregation in nine mammalian species: reference values and comparison of data. *Exp. Physiol.* 88, 431–440.
 71. Folch, J., Lees, M., and Sloane Stanley, G.H. (1957). A simple method for the isolation and purification of total lipides from animal tissues. *J. Biol. Chem.* 226, 497–509.
 72. Brown, R.J., Shao, F., Baldán, A., Albert, C.J., and Ford, D.A. (2013). Cholesterol efflux analyses using stable isotopes and mass spectrometry. *Anal. Biochem.* 433, 56–64.
 73. Liebisch, G., Binder, M., Schifferer, R., Langmann, T., Schulz, B., and Schmitz, G. (2006). High throughput quantification of cholesterol and cholesteryl ester by electrospray ionization tandem mass spectrometry (ESI-MS/MS). *Biochim. Biophys. Acta* 1761, 121–128.
 74. Tsukada, T., Rosenfeld, M., Ross, R., and Gown, A.M. (1986). Immunocytochemical analysis of cellular components in atherosclerotic lesions. Use of monoclonal antibodies with the Watanabe and fat-fed rabbit. *Arteriosclerosis* 6, 601–613.
 75. Pospisil, R., Kabat, J., and Mage, R.G. (2009). Characterization of rabbit CD5 isoforms. *Mol. Immunol.* 46, 2456–2464.
 76. Tsukada, T., Tippens, D., Gordon, D., Ross, R., and Gown, A.M. (1987). HHF35, a muscle-actin-specific monoclonal antibody. I. Immunocytochemical and biochemical characterization. *Am. J. Pathol.* 126, 51–60.
 77. Cybulsky, M.I., and Gimbrone, M.A., Jr. (1991). Endothelial expression of a mononuclear leukocyte adhesion molecule during atherogenesis. *Science* 251, 788–791.